ISSN 2616-5767 Vol.8, Issue 2: 68-75, DOI: 10.25236/AJETS.2025.080209

Modeling and Experimental Study on Rigid-flexible Coupling Dynamics of Missile Road Transportation

Yongyong Yan[1,a,*], Qihui Ling[1,b], Zeyu Li[1,c]

[1]*School of Mechanical Engineering, Hunan University of Science and Technology, Xiangtan, 411201, China*
[a]*2579566137@qq.com,* [b]*lqh_hunan@163.com,* [c]*15297328619@163.com*
**Corresponding author*

Abstract: *In order to analyze the dynamic characteristics of the missile road transportation system, a multi-body coupled dynamics model is constructed for "transportation vehicle - packing box - bomb body - missile component". Firstly, the dynamic model of transportation vehicle and missile components is established according to Newton's second law, the missile body is divided into three units, the flexible body dynamic model is established based on the theory of Euler-Bernoulli beam with variable cross section and the finite unit method, and the rigid-flexible coupling dynamics equations of "Transportation Vehicle-Packing Box-Bullet-Missile Components" are constructed through the principle of matching the degrees of freedom, and the state-space equations are deduced. Then, the model parameters are determined and the numerical simulation model is constructed using Matlab/Simulink platform. Finally, the sinusoidal sweep test is carried out on the road simulation test bed for model validation. The test results show that the displacement curves and amplitude-frequency characteristic curves are in good agreement, and the simulation peak errors at 3Hz and 5Hz frequencies are 1.67% and 2.83%, respectively, and the root-mean-square errors are 1.88% and 4.95%, respectively, which verifies the validity of the model. The model provides a reliable theoretical basis for the evaluation of the dynamic characteristics and optimal design of the missile road transportation system.*

Keywords: *Missile road transportation, Sine sweep frequency test, Numerical simulation, Model validation, Amplitude-frequency characteristic*

1. Introduction

As a high-precision strategic weapon system, missiles face a dynamic environment during transportation that directly affects the structural integrity and component reliability of the equipment [1]. Under the stimulation of complex road conditions, the multi-physical field coupling effect between the transportation carrier[2], buffer package and the body structure[3] may trigger potential risks such as resonance of the body structure and fatigue damage of precision components. Traditional research focuses on the dynamic analysis of a single transportation vehicle or cartridge structure, while ignoring the coupling mechanism of the multi-level system of "transportation vehicle-package-cartridge-component". Existing dynamics modeling methods face a double challenge when dealing with variable-section elastomers[4] and multi-body coupled systems[5]: on the one hand, the traditional centralized mass model is difficult to accurately characterize the distributed elasticity of the cartridge structure[6]; on the other hand, the time-varying nature of the interfacial force transfer between the subsystems puts forward the demand for higher-order nonlinear solutions in multi-body coupling modeling[7]. Despite the progress of the finite element method in the field of structural dynamics, its computational efficiency bottleneck in real-time simulation of complex transportation systems has not yet been effectively broken.

Aiming at the above problems, this study proposes a multiscale dynamics analysis method based on hybrid modeling theory, which constructs a coupled system dynamics model with engineering practical value by integrating the theory of Euler-Bernoulli beams of variable cross-section and the finite element discretization technique. This paper innovatively establishes a coupled dynamics architecture containing four-level subsystems, and distinguishes it from the conventional rigid-flexible coupling modeling method[8] by adopting a segmented elastomer discretization strategy, which ensures the computational accuracy and significantly reduces the model order at the same time. Through the construction of state space equations and Simulink real-time simulation platform, a complete technology chain from theoretical modeling to engineering verification is formed. The results of the study not only provide a

ISSN 2616-5767 Vol.8, Issue 2: 68-75, DOI: 10.25236/AJETS.2025.080209

new method to evaluate the dynamic characteristics of the missile transportation system, but also establish a reliable analytical framework for the optimal design of the transportation working conditions and the matching of buffer device parameters[9]. This system-level modeling idea has universal reference value for the study of heavy equipment transportation dynamics.

2. Dynamics Model of Missile Road Transportation

2.1 Simplification of Missile Road Transport System

The missile body[10] is divided into three units according to the modal state of the missile(Fig.1). Let the total length of the beam of the projectile body be *L*, the length of the discretized beam cell be l , and l_j denote the length of the jth beam cell.

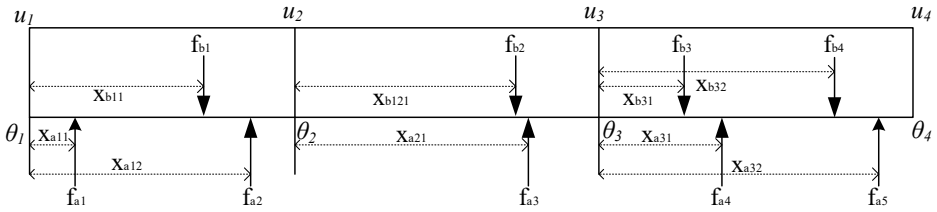

Figure.1 Structure model of elastic body beam.

In the figure, x_{aji} is the horizontal distance of the *i*th projectile support from the left end of the projectile beam *j* cell; x_{bji} is the horizontal distance of the *i*th missile component support from the left end of the projectile beam *j* cell; $u_1, \theta_1, \ldots, u_4, \theta_4$ is the vertical and angular displacements of the node of the *j*th beam cell, respectively. The finite element model adopts the consistent mass matrix of the beam cell.

The transportation vehicle dynamics were modeled using a two-axis, four-degree-of-freedom semi-vehicle model[11] (Fig. 2). The model considers four core degrees of freedom, including the vibration of each of the front and rear wheels in the vertical direction, the vertical vibration of the vehicle body and the pitching motion of the vehicle. This enables the model to analyze in depth the dynamic response of vehicles in complex road transportation environments. Moreover, the model also takes into account the time delay effect of the vehicle due to the difference in axle distance and traveling speed during the driving process. This effect leads to a significant difference in the road surface unevenness excitation experienced by the front and rear wheels. By incorporating this realistic factor, the model is able to more accurately simulate how the road surface excitation affects the main dynamic behaviors of the vehicle in the droop and pitch directions during real road transportation.

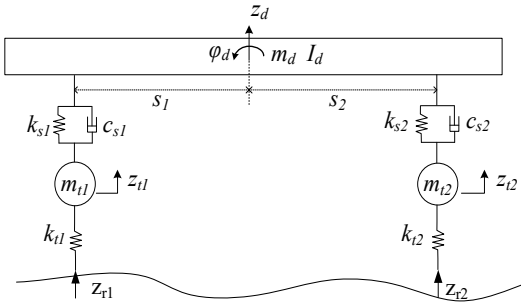

Figure.2 Two-axis four-degree-of-freedom half-car model.

The missile components are connected and fixed to the body by fasteners, and are subject to vibration transmission from the body during missile transportation. The main components are modeled as single-degree-of-freedom vibration models. The packing box is approximated as a rigid body for kinetic modeling; the support material of the projectile body is EVA foam, which has a certain degree of softness and vibration damping, so it is equivalent to a spring-damping system. In the actual missile road transportation process, the box will be fixed to the body of the car through the fixed parts.

ISSN 2616-5767 Vol.8, Issue 2: 68-75, DOI: 10.25236/AJETS.2025.080209

2.2 Coupling Dynamic Modeling of "Transport Vehicle-packaging Box-missile Body-missile Components"

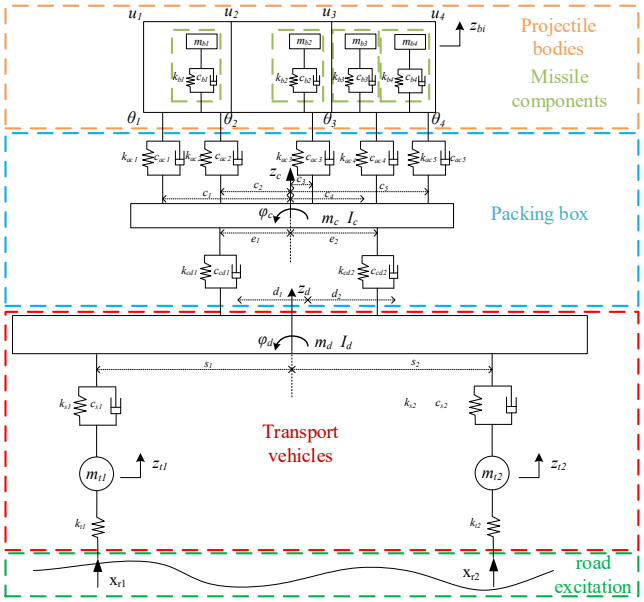

Figure.3 Coupling dynamics model of transport vehicle-package-body-missile components.

The coupled dynamics model of "transportation vehicle - packing box - bullet - missile component" (Fig.3). In the figure, m_d is the mass of the transportation vehicle; I_d is the rotational inertia of the transportation vehicle around its center of mass; s_1 and s_2 are the horizontal distances from the front and rear suspension of the transportation vehicle to the center of mass; k_{s1} and k_{s2} are the stiffness coefficients of the front and rear suspensions of the transportation vehicle; c_{s1} and c_{s2} are the damping coefficients of the front and rear suspensions of the transportation vehicle; m_{t1} and m_{t2} are the masses of front and rear wheels; k_{t1} and k_{t2} are the stiffness coefficients of front and rear wheels; x_{r1} and x_{r2} are the road surface unevenness excitation of the front and rear wheels; m_c is the mass of the packing box; I_c is the rotational moment of inertia of the packing box around its center of mass; d_1 and d_2 are the horizontal distances from the front and rear supports of the packing box to the center of mass of the transport vehicle; e_1 and e_2 are the horizontal distances from the front and rear supports of the packing box to its center of mass; k_{cd1} and k_{cd2} are the stiffness coefficients of the front and rear supports of the packing box; c_{cd1} and c_{cd2} are the damping coefficients of the front and rear supports of the packing box; k_{aci} is the stiffness coefficient of the support of the projectile body; c_{aci} is the damping coefficient of the support of the projectile body; m_{bi} is the mass of the missile component; k_{bi} is the stiffness coefficient of the missile component; c_{bi} is the damping coefficient of the missile component. The specific derivation process is as follows:

The dynamic equations for the wheels of the transportation vehicle are obtained from Newton's second law

$$M_t\ddot{Z}_t - C_sH_s\dot{Z}_d + C_s\dot{Z}_t - K_sH_sZ_d + \left(K_t + K_s\right)Z_t = K_tX_r \tag{1}$$

where M_t is the mass matrix of the transportation vehicle wheel; Z_t is the vibration displacement vector at the center of mass of the wheel of the transport vehicle; K_s and C_s are the stiffness matrix and damping matrix of the suspension of the transportation vehicle, respectively; K_t is the stiffness matrix of the transportation vehicle wheel; Z_r is the pavement unevenness matrix.

Similarly, the kinetic equations for the body of the transportation vehicle can be obtained

$$\begin{aligned} &M_d\ddot{Z}_d - H_d{}^TC_{cd}H_e\dot{Z}_c + \left(H_s{}^TC_sH_s + H_d{}^TC_{cd}H_d\right)\dot{Z}_d - H_s{}^TC_s\dot{Z}_t \\ &-H_d{}^TK_{cd}H_eZ_c + \left(H_s{}^TK_sH_s + H_d{}^TK_{cd}H_d\right)Z_d - H_s{}^TK_sZ_t = 0 \end{aligned} \tag{2}$$

where M_d is the mass matrix of the transportation vehicle body; Z_d is the vibration displacement vector of the center of mass of the transportation vehicle body; Z_c is the vibration displacement vector of the center of mass of the packing box; K_{cd} and C_{cd} are the stiffness matrix and damping matrix of the packing box support, respectively; H_d denotes the position matrix of the point of action of the packing box support

ISSN 2616-5767 Vol.8, Issue 2: 68-75, DOI: 10.25236/AJETS.2025.080209

with the transportation vehicle body; H_e denotes the position matrix of the point of action of the packing box support and the packing box. H_s denotes the position matrix of the point of action of the suspension of the transportation vehicle with the transportation vehicle body.

The dynamic equations of the transportation vehicle are obtained by combining equations (1) and (2)

$$M_v\ddot{Z}_v + C_v\dot{Z}_v + K_vZ_v = E_vZ_r \tag{3}$$

where M_v is the mass matrix of the transportation vehicle; Z_v is the vibration displacement vector of the center of mass of the body of the transportation vehicle; C_v and K_v are the damping matrix and stiffness matrix of the transportation vehicle.

The kinetic equations of the missile components are obtained from Newton's second law

$$M_b\ddot{Z}_b - C_bH_b\dot{Z}_a + C_b\dot{Z}_b - K_bH_bZ_a + K_bZ_b = 0 \tag{4}$$

Where M_b is the mass matrix of the missile components; Z_b is the vibration displacement vector of the missile component; Z_a is the nodal vibration displacement vector of the beam unit; C_b and K_b are the missile component damping and stiffness matrices, respectively; H_b denotes the position matrix of the missile component support at the point of action of the projectile.

The Euler-Bernoulli beam model[12] was used to simulate the dynamics of the elastic body

$$\alpha\frac{\partial^2}{\partial t^2}u(x,t) + c\frac{\partial}{\partial t}u(x,t) + EI\frac{\partial^4}{\partial x^4}u(x,t) = \sum f_i(t)\delta(x-l_i) \tag{5}$$

where α, c and EI denote the linear density, damping coefficient and bending stiffness of the projectile beam structure, respectively; $u(x,t)$ is the displacement response of the projectile beam at the moment x at t; f_{ai} is the force of the first projectile support on the projectile; and f_{bi} is the force of the first missile component on the projectile.

Elastomeric beam unit discrete-square model obtained by finite element method

$$M_a\ddot{Z}_a + C_a\dot{Z}_a + K_aZ_a = H_a{}^TF_a - H_b{}^TF_b \tag{6}$$

where M_a is the mass matrix of the elastic body beam; Z_a is the nodal vibration displacement vector of the beam unit; C_a and K_a are the damping matrix and stiffness matrix of the elastomeric beam, respectively; H_a denotes the position matrix of the projectile support at the point of action of the projectile; F_a denotes the matrix of the interaction force of the projectile support and the projectile; F_b denotes the matrix of the interaction force matrix of the missile component and the projectile body.

The kinetic equations of the elastic body are obtained by combining equations (4) and (6)

$$\begin{aligned} &M_a\ddot{Z}_a + \left(C_a + H_a{}^TC_{ac}H_a + H_b{}^TC_bH_b\right)\dot{Z}_a - H_b{}^TC_b\dot{Z}_b - H_a{}^TC_{ac}H_c\dot{Z}_c \\ &+\left(K_a + H_a{}^TK_{ac}H_a + H_b{}^TK_bH_b\right)Z_a - H_b{}^TK_bZ_b - H_a{}^TK_{ac}H_cZ_c = 0 \end{aligned} \tag{7}$$

where Z_c is the vibration displacement vector of the center of mass of the packing box; K_{ac} and C_{ac} are the stiffness and damping matrices of the elastomeric support; H_c denotes the position matrix of the elastomeric support with respect to the point of action of the packing box.

The kinetic equation of the packing box is obtained from Newton's second law

$$\begin{aligned} &M_c\ddot{Z}_c - H_c{}^TC_{ac}H_a\dot{Z}_a + \left(H_c{}^TC_{ac}H_c + H_e{}^TC_{cd}H_e\right)\dot{Z}_c - H_e{}^TC_{cd}H_d\dot{Z}_d \\ &-H_c{}^TK_{ac}H_aZ_a + \left(H_c{}^TK_{ac}H_c + H_e{}^TK_{cd}H_e\right)Z_c - H_e{}^TK_{cd}H_dZ_d = 0 \end{aligned} \tag{8}$$

Where M_c is the mass matrix of the packing box.

According to the principle of matching degrees of freedom, the coupled kinetic equations are obtained

$$M\ddot{Z} + C\dot{Z} + KZ = EZ_r \tag{9}$$

where M, C and K are the mass, damping and stiffness matrices of the coupled equations; Z is the vibrational displacement vector of the coupled equations.

Rewriting this equation as a state space equation

ISSN 2616-5767 Vol.8, Issue 2: 68-75, DOI: 10.25236/AJETS.2025.080209

$$\begin{cases} \dot{X} = AX + BX_r \\ Y = PX + QX_r \end{cases} \tag{10}$$

where the state variable

$$X = \begin{pmatrix} Z & \dot{Z} \end{pmatrix}^T \tag{11}$$

Output variable

$$Y = \begin{pmatrix} Z & \dot{Z} & \ddot{Z} \end{pmatrix}^T \tag{12}$$

Specific expressions for the matrix A、B、P、Q

$$A = \begin{pmatrix} 0 & 1 \\ -\frac{M}{K} & -\frac{M}{C} \end{pmatrix} \tag{13}$$

$$B = \begin{pmatrix} 0 \\ \frac{M}{E} \end{pmatrix} \tag{14}$$

$$P = \begin{pmatrix} 1 & 0 & 0 & 0 & 0 & 0 & 0 & 0 & 0 & 0 \\ 0 & 1 & 0 & 0 & 0 & 0 & 0 & 0 & 0 & 0 \\ 0 & 0 & 1 & 0 & 0 & 0 & 0 & 0 & 0 & 0 \\ 0 & 0 & 0 & 1 & 0 & 0 & 0 & 0 & 0 & 0 \\ 0 & 0 & 0 & 0 & 1 & 0 & 0 & 0 & 0 & 0 \\ 0 & 0 & 0 & 0 & 0 & 1 & 0 & 0 & 0 & 0 \\ 0 & 0 & 0 & 0 & 0 & 0 & 1 & 0 & 0 & 0 \\ 0 & 0 & 0 & 0 & 0 & 0 & 0 & 1 & 0 & 0 \\ 0 & 0 & 0 & 0 & 0 & 0 & 0 & 0 & 1 & 0 \\ 0 & 0 & 0 & 0 & 0 & 0 & 0 & 0 & 0 & 1 \\ -\frac{M_a}{K_a + H_a^T K_{ac} H_a + H_b^T K_b H_b} & \frac{M_a}{H_b^T K_b} & \frac{M_a}{H_a^T K_{ac} H_c} & 0 & 0 & -\frac{M_a}{C_a + H_a^T C_{ac} H_a + H_b^T C_b H_b} & \frac{M_a}{H_b^T C_b} & \frac{M_a}{H_a^T C_{ac} H_c} & 0 & 0 \\ \frac{M_b}{K_b H_b} & \frac{M_b}{K_b} & 0 & 0 & 0 & \frac{M_b}{C_b H_b} & -\frac{M_b}{C_b} & 0 & 0 & 0 \\ \frac{M_c}{H_c^T K_{ac} H_a} & 0 & -\frac{M_c}{H_c^T K_{ac} H_c + H_r^T K_{cd} H_r} & \frac{M_c}{H_r^T K_{cd} H_d} & 0 & \frac{M_c}{H_c^T C_{ac} H_a} & 0 & -\frac{M_c}{H_c^T C_{ac} H_c + H_r^T C_{cd} H_r} & \frac{M_c}{H_r^T C_{cd} H_d} & 0 \\ 0 & 0 & \frac{M_d}{H_d^T K_{cd} H_c} & -\frac{M_d}{H_r^T K_r H_r + H_d^T K_{cd} H_d} & \frac{M_d}{H_r^T K_r} & 0 & 0 & \frac{M_d}{H_d^T C_{cd} H_c} & -\frac{M_d}{H_r^T C_r H_r + H_d^T C_{cd} H_d} & \frac{M_d}{H_r^T C_r} \\ 0 & 0 & 0 & \frac{M_t}{K_t H_t} & -\frac{M_t}{K_t + K_t} & 0 & 0 & 0 & \frac{M_t}{C_t H_t} & -\frac{M_t}{C_t} \end{pmatrix} \tag{15}$$

$$Q = \begin{pmatrix} 0 & 0 & 0 & 0 & 0 & 0 & 0 & 0 & 0 & 0 & 0 & 0 & 0 & 0 & \frac{M_t}{K_t} \end{pmatrix}^T \tag{16}$$

3. Model Parameter

The projectile model parameters are obtained through the mass, size and material data of the model projectile; the vehicle model parameters are obtained based on the tests done by the group in the past; the missile component support, projectile support and packing box support are obtained based on the finite element simulation software, taking the projectile support as an example, and the specific process is as follows:

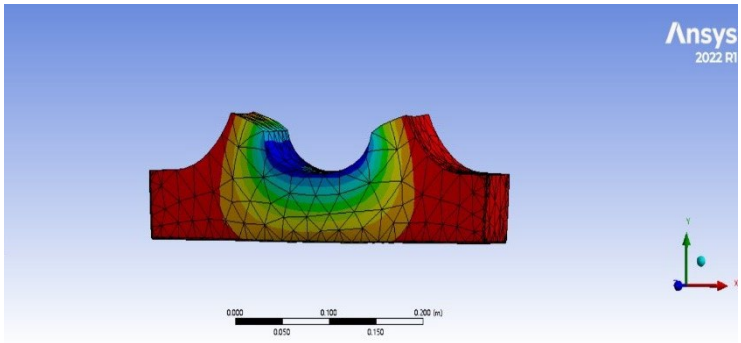

Figure.4 Finite element model of projectile body support.

The projectile model parameters are obtained by the mass, size and material data of the model bomb; the vehicle model parameters are obtained based on the tests done by the group in the past; the missile component support, projectile support and packing box support are obtained based on the finite element

ISSN 2616-5767 Vol.8, Issue 2: 68-75, DOI: 10.25236/AJETS.2025.080209

simulation software, taking the projectile support as an example, the density of the EVA foam is 0.25g/cm^3, the modulus of elasticity is 5Mpa, and Poisson's ratio is taken as 0.3, and a three-dimensional model of the projectile support is established by the Solidworks software, and a force of 100-1000N is applied on the contact surface with the finite element model to get the support. software to establish a three-dimensional model of the elastomer support, and finite element model joint simulation (Fig.4), in the elastomer support on the contact surface of the elastomer support to apply 100-1000N force, to get the elastomer support deformation variables, and finally according to the elasticity of the elastic force formula fitting to get the elastomer support equivalent stiffness value.

After determining the elastomeric support stiffness, the intrinsic frequency of the elastomeric beam model with support constraints is calculated based on the eigenvalues of the mass matrix and stiffness matrix corresponding to the elastomeric degrees of freedom. Assuming that the first two orders of modal damping ratio is 0.02, according to the modal analysis of the elastomer with support constraints done by the group, the first two orders of the intrinsic frequency are 114 Hz and 152 Hz, and the Rayleigh damping coefficient of the elastomeric beam model can be solved by using the obtained intrinsic frequency.

4. Test Verification

4.1 Sinusoidal Excitation Sweep Frequency Test

In order to verify the validity of the coupled dynamics model, a certain type of micro truck, packing box and model bullet are used as application examples, and the road simulation test platform is utilized to carry out the sinusoidal excitation sweeping test with a frequency of 1-20 Hz (Fig.5). The main components of the test include: hydraulic shaker, test vehicle, packing box, model bullet, control system, vibration test system, sensors and signal lines.

Figure.5 Missile transportation sweep frequency test.

Through the shaker to the test system to provide 1-20Hz frequency sinusoidal sweep excitation signal, to be the system response stabilized, to get the focus of the projectile body (measurement point) vertical acceleration response test data. Then the acceleration response is converted into displacement response by LabGenius software.

4.2 Comparative Analysis of Simulation and Test Results

The coupled dynamics simulation model (Fig.6) constructed in Matlab/Simulink platform[13], the sinusoidal swept signal used during the test is used as the input of the coupled dynamics model for numerical simulation, and the dynamic displacement responses of measurement point is obtained.

By comparing the amplitude-frequency characteristic curves of the experimental data and simulation data(Fig.7), it is found that the two present a resonance peak near the 3Hz frequency. To further verify the model accuracy, the response values at 3Hz and 5Hz frequencies are extracted for comparative analysis(Fig.8-9).

ISSN 2616-5767 Vol.8, Issue 2: 68-75, DOI: 10.25236/AJETS.2025.080209

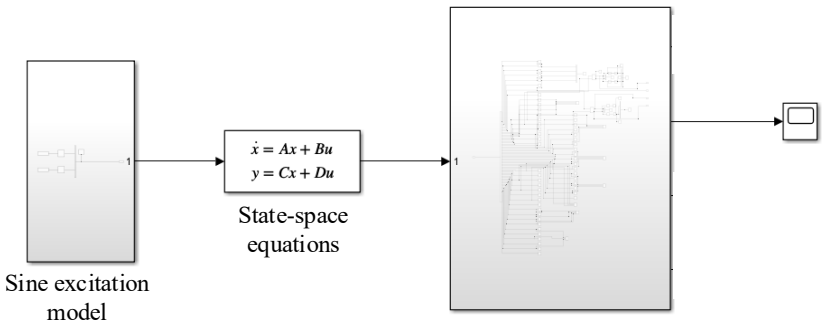

Figure.6 Simulation model.

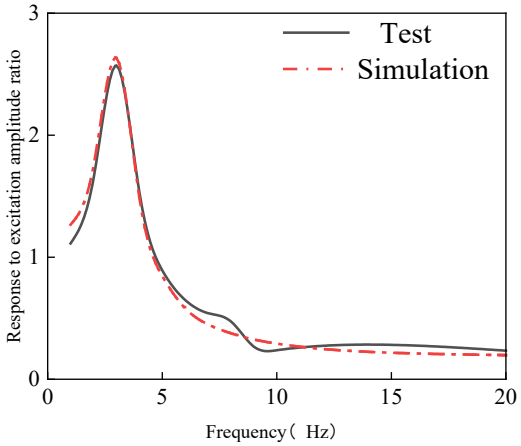

Figure.7 Comparison of amplitude frequency characteristic curves.

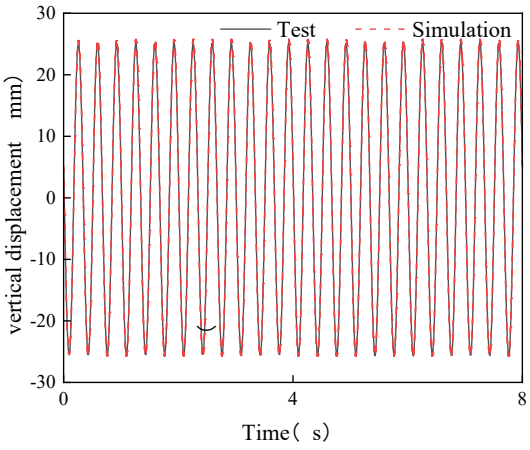

Figure. 8 Comparison of vertical displacement at 3Hz frequency.

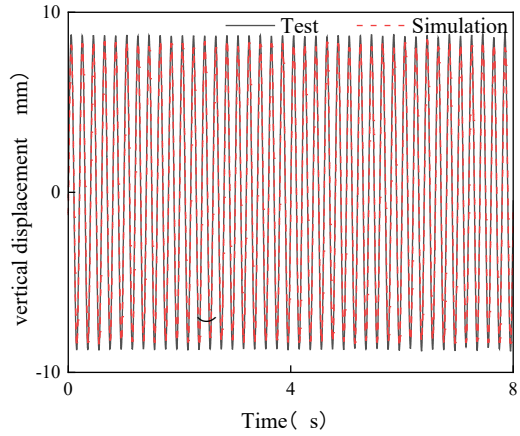

Figure. 9 Comparison of vertical displacement at 5Hz frequency.

ISSN 2616-5767 Vol.8, Issue 2: 68-75, DOI: 10.25236/AJETS.2025.080209

Table.1 Root mean square value of vertical displacement.

Frequency (Hz)	Simulation	Test	Relative error/%
3	18.24	17.91	1.88
5	5.79	6.09	4.95

The root mean square values of vertical displacement at different frequencies are shown in Table 1. It is found that when the sinusoidal excitation frequency is 3hz, the peak simulation errors of measurement point is 1.67%, and the root mean square relative errors is 1.88%. When the sinusoidal excitation frequency is 5hz, the simulated peak errors of measurement point increase to 2.83%, and the root mean square relative errors increase to 4.95%. The comparison reveals that the simulation and experimental results are in good agreement, indicating that the established coupled dynamics model can effectively characterize the dynamic transfer characteristics of the missile road transportation system.

5. Conclusion

(1) According to Newton's second law to establish the dynamic model of the transportation vehicle, missile components and packing box, the bullet body is divided into three units, based on the theory of Euler-Bernoulli beams with variable cross section and the finite unit method to establish the dynamic model of the flexible body, and through the principle of matching the degrees of freedom to construct the rigid-flexible coupled dynamic equations of the “transportation vehicle-packing box-bullet-body-missile components” and to derive the state-space equations. (2) Sine excitation frequency sweeping test of 1-20Hz is carried out by using the road simulation test platform. The coupled dynamics simulation model was constructed in Matlab/Simulink platform, and the sinusoidal frequency sweep signal used in the test was used as the input of the coupled dynamics model for numerical simulation. (3) The amplitude-frequency characteristic curves of the test data and simulation data were compared with the displacement curves at 3 Hz and 5 Hz, the peak error and the root-mean-square relative error. It is found that the curves at the measurement points match well and the errors are small, indicating that the established coupled dynamics model can effectively characterize the dynamic transfer characteristics of the missile road transportation system.

References

[1] Lin S, Guo-Feng Z, Xin L U. Vibration Environment Condition for Highway and Off-road Transportation of Tactical Missile[J].Equipment Environmental Engineering, 2017..
[2] M A I,M A A, H K . Design and optimization of a missile transporter semi-trailer structure[J].Journal of Physics: Conference Series,2022,2299(1).
[3] Tianyang Z, Jiahao Z, Qingbo Y.Research on aerodynamic optimization of hypersonic missiles[J].IOP Publishing Ltd, 2024.DOI:10.1088/1742-6596/2891/11/112026.
[4] Liang W, Lin S, Le W. Study on the Structure Dynamic Modeling of Tactical Missile[J].Tactical Missile Technology, 2013.
[5] Liu Z, Wang G, Rui X, et al.Modeling and simulation framework for missile launch dynamics in a rigid-flexible multibody system with slider-guide clearance[J].Nonlinear Dynamics, 2024, (prepublish):1-28.
[6] Liang W, Huai-Hai C, Chang-Jian Z,et al.Research of dynamics of the beam with axial movement[J].Journal of Vibration Engineering,2016.DOI:10.16385/j.cnki.issn.1004-4523.2016.01.007.
[7] Wang X, Rui X, Yang F,et al.Launch Dynamics Modeling and Simulation of Vehicular Missile System[J].Journal of Guidance Control and Dynamics, 2018, 41(5):1-10.DOI:10.2514/1.G003363.
[8] Yonghui Z, Hongliang W, Jun L. Research on Dynamic Characteristics of Missile Launching System[J].Tactical Missile Technology, 2013.
[9] Jikun Y , Tingxue X , Haowei W ,et al.Research on Modeling Methods of Availability Based on Missile Weapon System[J].Tactical Missile Technology, 2012.
[10] Anmin Z, Lianhu C, Shiming Z .Study of three Degree of Freedom Tactical Missile Simulation Model[J].System Simulation Technology, 2016.
[11] Tang X, Yang K, Wang H,et al.Driving Environment Uncertainty-Aware Motion Planning f or Autonomous Vehicles[J]. Chinese Journal of Mechanical Engineering,2022, 35(5):120-120.DO I:10.1186/s10033-022-00790-5.
[12] Cao Z, Xue M A, Yuan X,et al.A fast semi-analytic solution of liquid sloshing in a 2-D tank with dual elastic vertical baffles and walls[J].Ocean Engineering, 2023. DOI:10.1016/j.oceaneng.2023.113951.
[13] Rui-Xin B, Sabbioni E. The Vehicle Dynamics and State Estimation Model Design Based on Matlab/Simulink[J].Computer Simulation, 2015.